Electron paramagnetic resonance of divalent thallium in cadmium telluride*

R. C. DuVarney and A. K. Garrison
Emory University, Atlanta, George 30322
(Received 9 December 1974)

An analysis of EPR spectra from CdTe:Tl single crystals shows that Tl^{2+} goes into the CdTe lattice as a substitutional impurity at a cadmium site. The unpaired s electron on the thallium ion has an isotropic hyperfine interaction of 53.3 ± 0.3 and 53.7 ± 0.3 GHz with the ^{203}Tl and ^{205}Tl isotopes, respectively, and a g factor of -2.035 ± 0.015. The sign of the hyperfine-interaction constant is inferred to be positive from the temperature dependence of the line intensities and the negative sign of the g factor is assumed. A superhyperfine (shf) interaction with the nearest-neighbor tellurium ligand ions is observed whenever the sites are occupied by the 7% abundant ^{125}Te nucleus. The shf-interaction tensor is axially symmetric about the bond direction with $|A_{\parallel}| = 375 \pm 5$ G and $|A_{\perp}| = 180 \pm 5$ G.

I. INTRODUCTION

Using electron paramagnetic resonance (EPR) to study single crystals of CdTe that have been purposely doped with various ions to cause charge compensation, we have found that CdTe doped with thallium gives EPR spectra at 77 °K. The spectra are characterized by a hyperfine interaction with the thallium nucleus, which is larger than the electron Zeeman interaction, and by a g factor near the free-electron value. Since paramagnetic Tl^{2+} ions have a $^2S_{1/2}$ ground state which would give rise to a large hyperfine interaction and small g shift, we conclude that the thallium enters the CdTe lattice as Tl^{2+}.

The EPR spectra also show a superhyperfine (shf) structure, which we attribute to the interaction of the thallium electron with nearest-neighbor (nn) tellurium isotopes with nuclear spin $I = \frac{1}{2}$. The analysis of the orientation dependence of the superhyperfine spectra shows that the Tl^{2+} ions are substitutional for Cd.

Räuber and Schneider[1] have reported an EPR study of Tl^{2+} in ZnS, and Dreybrodt and Silber[2] report a similar study in KCl. No other EPR studies of thallium in the zinc chalcogenides have been reported nor have any been previously reported in the corresponding cadmium compounds. The $^2S_{1/2}$ state ion Pb^{3+} has been studied by EPR in ZnO,[3] ZnSe,[4] and ZnTe,[5] but not in the cadmium compounds. Comparison of our data where possible indicates that the electron-spin density on the thallium decreases as it substitutes into more covalently bonded lattices. We are also able to predict the g shifts of Tl^{2+} in CdSe and CdS using the measured value in CdTe and the theory of Watanabe.[6]

II. EXPERIMENTAL TECHNIQUE

The single crystals used in this study were obtained from K. Zanio of Hughes Laboratories. The crystals were cleaved along {110} planes to form samples approximately 10 mm^3 in volume. Samples were mounted so that the external magnetic field could be rotated in a (110) plane. The data were taken on a Varian V-4500, X-band spectrometer equipped with a 9-in. magnet, field-regulated power supply, and 100-kHz lock-in detection. The external magnetic-field strength was measured with an Alpha-Scientific NMR proton probe and an HP 5246L frequency counter. This counter with an HP 5255A frequency converter was also used to measure the klystron frequency. The data were taken at 77 °K, employing a Varian insert Dewar in a V-4533 cylindrical cavity.

Experiments were also performed at 4 °K, using a rectangular cavity in an immersion Dewar. Superheterodyne detection at 30 MHz was employed, with the external magnetic field modulated at 400 Hz. No signals, however, were observed at this temperature.

The samples were placed in a Varian V-4531 Multi-Purpose Cavity, irradiated at 77 °K with band-gap light from a 750-W incandescent bulb and with unfiltered light from a 500-W Osram mercury lamp. In neither case were the EPR signals significantly altered.

III. RESULTS

The spectra, a typical example of which is shown in Fig. 1, consist of two sets of lines. The sets are about 2600 G apart and are centered at about 7000 G. Each set consists of an intense isotropic line surrounded symmetrically by weak anisotropic satellite lines. In the high-field spectrum, the central portion partially resolves into two lines with an intensity ratio of about 2:1. This agrees reasonably well with the relative abundance of the two naturally occurring thallium isotopes. ^{203}Tl is 29.5% abundant, while ^{205}Tl has an abundance of 70.5%. In the low-field spectrum the isotope splitting is not resolved. However that line is 50% wider than the partially resolved line in the high-

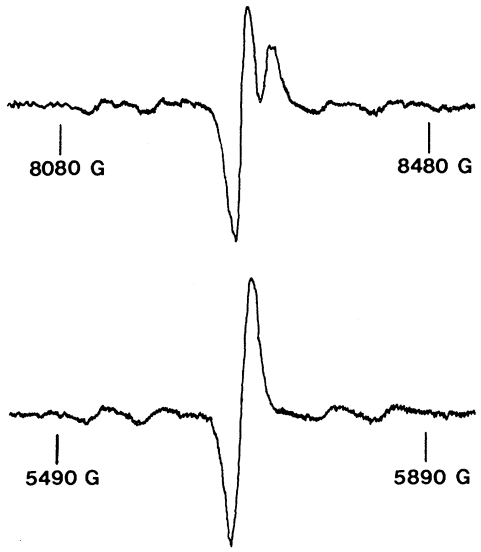

FIG. 1. The EPR spectrum of Tl^{2+} in CdTe at 77 °K with external magnetic field along a [110] direction. The Klystron frequency was 9283.4 MHz.

field set. The ratio between the intensity of the central line and the total intensity of the satellite lines can be seen from Fig. 1 to be about 3 : 1. This agrees well with a model in which the thallium impurity substitutes for a cadmium ion in the zinc-blende lattice of CdTe. Each thallium then would have four nn tellurium nuclei, and the unpaired electron which chiefly resides on the thallium ion could undergo a shf interaction with those tellurium ions that have nuclear magnetic moments. ^{125}Te and ^{123}Te both have nuclear spin-$\frac{1}{2}$, almost equal magnetic moments, and they occur with natural abundances of 7% and 1%, respectively. The remaining 92% have no magnetic moments at all. From this, one can calculate that approximately 72% of the thallium sites have no shf structure, while 25% of the sites would show a shf pattern due to one nn spin, and approximately 3% of the sites would exhibit a pattern due to two nn spins. The number of sites having three or four spin-$\frac{1}{2}$ neighboring nuclei would be negligibly small. In fact, sites having more than one nn spin give signals that are too weak to be observed in this experiment.

The spectra can be completely analyzed with the spin Hamiltonian,

$$H = ha\vec{S}\cdot\vec{I} - g\mu_B\vec{S}\cdot\vec{B} - g_N\mu_N\vec{I}\cdot\vec{B} - g\mu_B\vec{S}\cdot\overleftrightarrow{A}\cdot\vec{I}', \tag{1}$$

where a is the isotropic-hyperfine-interaction constant for the thallium nucleus in Hz, g is the electron g factor which, contrary to the usual sign convention in EPR, is taken as negative, g_N is the nuclear g factor for the thallium nucleus, $\overleftrightarrow{A}$ is the cylindrically symmetric shf interaction tensor for the tellurium nucleus in G, and μ_B and μ_N are the Bohr magneton and the nuclear magneton for the thallium nucleus, respectively. The shf interaction is not summed over the four neighboring tellurium nuclei because sites with more than one spin-$\frac{1}{2}$ tellurium nuclei were not observed, as explained above.

When the first term of Eq. (1) is largest, it describes a system where the electron is more strongly coupled to the central nucleus than to the external magnetic field. Using the presentation given by Ramsey[7] of the original Breit-Rabi[8] treatment of such a case, one gets the energy levels of the coupled system when the shf interaction is neglected as

$$W(F, m) = -\tfrac{1}{4}ha - g_N\mu_N B_0 m \pm \tfrac{1}{2}ha\,(1 + 2mz + z^2)^{1/2}, \tag{2}$$

where

$$z = (-g\mu_B + g_N\mu_N)B_0/ha\ .$$

Here F takes on the values $|I \pm S|$, which for our case is either 1 or 0, and m is the component of F along the external magnetic field. The "+" sign in Eq. (2) is chosen when $F = 1$, and the "−" sign for $F = 0$. The EPR transitions that we observed are within the $F = 1$ manifold, one from the state (1, 1) to (1, 0), and the other from (1, 0) to (1, −1). This fact is apparent from the temperature dependence of the resonance signals. At room temperature, the signals are too broad to be observed. At 77 °K they are narrow enough to be observed, but at 4.2 °K there is no absorption at all. This indicates that the levels of the $F = 1$ manifold are higher than the $F = 0$ levels, and that the EPR transitions are within the $F = 1$ manifold. The sign of a is inferred to be positive from this result.

The hyperfine-coupling constant may be expressed in terms of the two external magnetic fields B_1 and B_2 that satisfy the resonance condition at a fixed klystron frequency ν. This expression is:

$$\frac{a}{\nu} = -\frac{B_1x + B_2y}{B_1 - B_2} \pm \left(\frac{(B_1x + B_2y)^2}{(B_1 - B_2)^2} + \frac{2(B_1x' - B_2y')}{B_1 - B_2}\right)^{1/2}, \tag{3}$$

where $B_2 > B_1$ and

$$x = (\tfrac{1}{2} + B_1/C + B_1B_2/2C^2)\ ;\quad y = (\tfrac{1}{2} + B_2/C + B_1B_2/2C^2)\ ;$$

$$x' = (1 + B_1/C + B_1B_2/C^2)\ ;\quad y' = (1 + B_2/C + B_1B_2/C^2)$$

with $C = h\nu/2g_N\mu_N$.

One also can show that

$$-g\mu_B + g_N\mu_N = \frac{h\nu}{B_1}\,\frac{(1 + B_1/C)\,(1 + B_1/C + a/\nu)}{1 + B_1/C + a/2\nu}, \tag{4}$$

or equivalently,

TABLE I. Computed spin-Hamiltonian parameters for Tl^{2+} in CdTe.

	a (GHz)	g	$\lvert A_{\parallel}\rvert$ (G)	$\lvert A_{\perp}\rvert$ (G)
^{203}Tl	53.3 ± 0.3[a]	-2.035 ± 0.015[b]	375 ± 5	180 ± 5
^{205}Tl	53.7 ± 0.3[a]	-2.035 ± 0.015[b]	375 ± 5	180 ± 5

[a]Positive sign of a has been inferred from the temperature dependence of the line intensities.

[b]Sign of g is assumed to be negative.

$$-g\mu_B + g_N\mu_N = \frac{h\nu}{B_2}\,\frac{(1+B_2/C)\,(1+B_2/C-a/\nu)}{1+B_2/C-a/2\nu}\,. \qquad (5)$$

Equations (3), (4), and (5) reduce to the corresponding expressions given by Dreybrodt and Silber[2] if one neglects terms of order B/C and B^2/C^2 in the expressions for x, y, x', and y'.

In applying these expressions to the data analysis, it was found that terms involving C^2 could be neglected in evaluating the hyperfine-coupling constants and g value. The accuracy of the hyperfine-coupling constants a for Tl is limited by the linewidth, and since this error in a is the main contribution to the error in the calculation of the g factor from Eq. (4) or (5), the accuracy of the g factor is lower than normally obtained in EPR measurements. Because of this, using a higher microwave frequency would not improve the accuracy in the g-factor measurements, as in the usual case. The results are given in Table I.

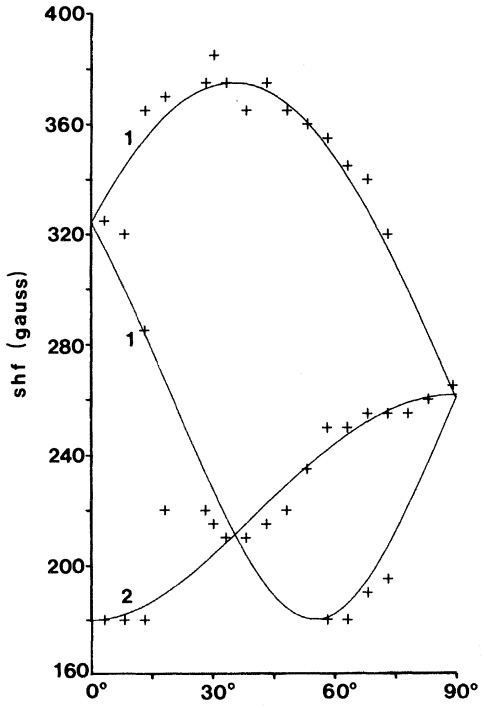

FIG. 2. The angular dependence of the ^{125}Te shf splitting with the magnetic field rotated in one of the {110} planes. 0° corresponds to the magnetic field parallel to one of the ⟨110⟩ directions. The crosses are the measured values, and the solid lines were calculated from Eq. (6) using the values in Table I. The numbers 1 or 2 near each of the calculated curves give the theoretical relative intensity of the lines.

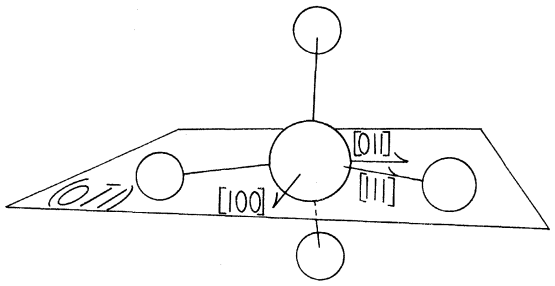

FIG. 3. A schematic showing the orientations of the four nn tellurium bond directions with respect to a (0$\bar{1}$1) plane and with respect to the principal directions contained in that plane. The large circle represents the Tl^{2+} impurity, and the four smaller circles represent the tellurium ligands.

In analyzing the shf structure, we have assumed that the interaction tensor is cylindrically symmetric with its axis of symmetry along the appropriate nn tellurium bond direction. Although the interaction of the tellurium nucleus with the unpaired electron is much greater than the interaction of the tellurium nucleus with the external magnetic field, it is much smaller than both the hyperfine interaction of the unpaired electron with the thallium nucleus and the electronic Zeeman interaction. The shf interaction, then, can be thought of as a perturbation on the external field, and the splitting of the satellite lines in G can be expressed to first order as

$$\Delta B = (A_{\parallel}^2\cos^2\theta + A_{\perp}^2\sin^2\theta)^{1/2}\,. \qquad (6)$$

Here θ is the angle between the appropriate nn tellurium bond direction and the direction of the external magnetic field. Figure 2 shows the splitting of the satellite lines as a function of crystal orientation with respect to the external field direction. The magnetic field is constrained to move in a (110) plane. The crosses are the measured line positions, and the solid lines are calculated from Eq. (6), using the values of $\lvert A_{\perp}\rvert$ and $\lvert A_{\parallel}\rvert$ given in Table I. Although care was taken to optimize spectrometer sensitivity, these satellite lines were weak and rather broad. Orientations at which there are fewer crosses than predicted lines are those for which all the lines are not resolved. The numbers 1 or 2 near each of the calculated curves in Fig. 2 give the theoretical relative intensity for that line. The observed intensity of the satellite lines were consistent with these designations. Fig-

TABLE II. Values for the spin density at the nucleus and the g factor for Tl^{2+} in various host crystals.

	Free ion	KCl[a]	ZnS[b]	CdTe[c]
$\lvert\psi(0)\rvert^2$ $(10^{24}/cm^3)$	459	275	187	138
$\lvert g\rvert$	2.002	2.010	2.0095	2.035

[a]W. Dreybrodt and D. Silbert (Ref. 2).
[b]A. Räuber and J. Schneider (Ref. 1).
[c]This work.

ure 3 shows the orientation of the four nearest-neighbor tellurium bond directions with respect to a (110) plane and the principal directions contained in that plane. A simple comparison of the two figures shows that the model of the impurity as shown in Fig. 3 is completely compatible with the symmetry and angular dependence displayed by the data.

IV. DISCUSSION

The use of purposely doped crystals, the uniqueness of the Tl isotope effect, the consistency of the analyses using the Breit-Rabi case, the temperature dependence of the EPR line intensity, and the Tl shf structure all seem to us to be strong support for the conclusion that we are observing Tl^{2+} in a substitutional site and to preclude the necessity of measurement at another microwave frequency to establish this model.

Some results of studies on Tl^{2+} in other materials are given in Table II. One obvious trend is seen in the reduction of the unpaired spin density at the nucleus, and hence, the hyperfine coupling as the bonding within the host lattice becomes more covalent.

It is also interesting to compare the g shift of Tl^{2+} in CdTe to those of Pb^{3+} in the zinc chalcogenide series. Born *et al.*[9] have applied the Watanabe theory for the S-state ion g shift[6] in which Δg is proportional to the spin-orbit coupling constant λ for the ligand ions surrounding the impurity in the various host lattices. They show that this relationship holds for Pb^{3+} in the zinc chalcogenide series where the greatest g shift is observed in ZnTe. Applying this same analysis to Tl^{2+} in the cadmium chalcogenide series and taking our measurement of $+0.033 \pm 0.015$ as the g shift of Tl^{2+} in CdTe, one estimates a g shift of $+0.015 \pm 0.008$ for Tl^{2+} in CdSe and $+0.003 \pm 0.002$ for the g shift in CdS. The uncertainty in these estimates has been obtained by scaling the uncertainty in our measurement in the same proportion that the g shift is scaled. These estimates are based on the values of λ for neutral atoms of S, Se, and Te listed by Watanabe[6] and the assumption that the ratios of λ for the ions is the same as the free ions. To our knowledge, measurements of these g shifts have not been reported. These results are summarized in Table III.

TABLE III. Comparison of the g shift for Tl^{2+} in the cadmium chalcogenides with the g shift for Pb^{3+} in the zinc chalcogenides.

X	S	Se	Te
λ (cm^{-1})	352–396	1868	4203
g shift for Tl^{2+} in CdX	$+0.003 \pm 0.002$[a]	$+0.015 \pm 0.008$[a]	$+0.033 \pm 0.015$[b]
g shift for Pb^{3+} in ZnX	$+0.015$[a]	$+0.071$[c]	$+0.165$[c]

[a]Predicted from the theory of Watanabe.
[b]Based on measurement reported in this paper.
[c]Taken from the measurements made by Born *et al.* (Ref. 9).

One would also expect the spin density at the nucleus and hence the hyperfine coupling to bear some form of inverse relationship to the g shift. Generally speaking, the greater the g shift, the less central s character the molecular orbital will have and hence, a smaller hyperfine coupling. Thus for Tl^{2+} in the cadmium chalcogenide series, the spin density should increase from 13×10^{24} cm^{-3} in CdTe where Δg is a maximum toward the free-ion value of 459×10^{24} cm^{-3} as Δg decreases. This is also shown in the work of Born *et al.*[9] in their correlation of the hyperfine splitting with the g shift of Pb^{3+} in the zinc chalcogenide series.

It is difficult to make further comparisons of our results with related experiments since so little information is available on S-state impurities in the cadmium chalcogenides or Tl^{2+} in other II-VI host crystals. It should be noted here that an initial search for EPR spectra in CdTe doped with boron, aluminum, or indium showed no signals from ions of these elements.

ACKNOWLEDGMENTS

The authors wish to thank K. Zanio for supplying the CdTe crystals doped with thallium, aluminum, and indium, and A. J. Strauss for supplying the CdTe crystals doped with boron.

*Work supported in part by U. S. Atomic Energy Commission Contract No. AT-(40-1)-4146.

[1]A. Räuber and J. Schneider, Phys. Status Solidi 18, 125 (1966).
[2]W. Dreybrodt and D. Silber, Phys. Status Solidi 20, 337 (1967).
[3]G. Born, A. Hofstaetter, and A. Scharmann, Z. Physik 240, 163 (1970).

[4]W. C. Holton and R. K. Watts, J. Chem. Phys. 51, 1615 (1969).
[5]K. Suto and M. Aoki, II-VI *Semiconducting Compounds* 1967 *Conference*, edited by D. G. Thomas (Benjamin, New York, 1967), p. 1359.
[6]H. Watanabe, Phys. Rev. 149, 402 (1966).
[7]N. F. Ramsey, *Molecular Beams* (Clarendon, Oxford, England, 1956), p. 120.
[8]G. Breit and I. I. Rabi, Phys. Rev. 38, 2082 (1931).
[9]G. Born, A. Hofstaetter, and A. Scharmann, Z. Physik 248, 7 (1971).